ACS Synthetic Biology

Subscriber access provided by SHANGHAI DOC & INFO CENTER

Article

Orthogonal genetic regulation in human cells using chemically induced CRISPR/Cas9 activators

Zehua Bao, Surbhi Jain, Valerie Jaroenpuntaruk, and Huimin Zhao

ACS Synth. Biol., **Just Accepted Manuscript** • DOI: 10.1021/acssynbio.6b00313 • Publication Date (Web): 05 Jan 2017

Downloaded from http://pubs.acs.org on January 13, 2017

Just Accepted

"Just Accepted" manuscripts have been peer-reviewed and accepted for publication. They are posted online prior to technical editing, formatting for publication and author proofing. The American Chemical Society provides "Just Accepted" as a free service to the research community to expedite the dissemination of scientific material as soon as possible after acceptance. "Just Accepted" manuscripts appear in full in PDF format accompanied by an HTML abstract. "Just Accepted" manuscripts have been fully peer reviewed, but should not be considered the official version of record. They are accessible to all readers and citable by the Digital Object Identifier (DOI®). "Just Accepted" is an optional service offered to authors. Therefore, the "Just Accepted" Web site may not include all articles that will be published in the journal. After a manuscript is technically edited and formatted, it will be removed from the "Just Accepted" Web site and published as an ASAP article. Note that technical editing may introduce minor changes to the manuscript text and/or graphics which could affect content, and all legal disclaimers and ethical guidelines that apply to the journal pertain. ACS cannot be held responsible for errors or consequences arising from the use of information contained in these "Just Accepted" manuscripts.

ACS Publications

ACS Synthetic Biology is published by the American Chemical Society. 1155 Sixteenth Street N.W., Washington, DC 20036

Published by American Chemical Society. Copyright © American Chemical Society. However, no copyright claim is made to original U.S. Government works, or works produced by employees of any Commonwealth realm Crown government in the course of their duties.

Submitted to *ACS Synthetic Biology*

Orthogonal genetic regulation in human cells using chemically induced CRISPR/Cas9 activators

Zehua Bao[1], Surbhi Jain[1], Valerie Jaroenpuntaruk[1] and Huimin Zhao[1,2,*]

[1] Department of Biochemistry, University of Illinois at Urbana-Champaign, Urbana, IL 61801

[2] Departments of Chemical and Biomolecular Engineering, Chemistry, and Bioengineering, Carl R. Woese Institute for Genomic Biology, University of Illinois at Urbana-Champaign, Urbana, IL 61801

* To whom correspondence should be addressed. Tel: (217) 333-2631; Fax: (217) 333-5052; Email: zhao5@illinois.edu

ABSTRACT

The concerted action of multiple genes in a time-dependent manner controls complex cellular phenotypes, yet the temporal regulation of gene expressions is restricted on a single gene level, which limits our ability to control higher order gene networks and understand the consequences of multiplexed genetic perturbations. Here we developed a system for temporal regulation of multiple genes. This system combines the simplicity of CRISPR/Cas9 activators for orthogonal targeting of multiple genes and the orthogonality of chemically induced dimerizing (CID) proteins for temporal control of CRISPR/Cas9 activator function. In human cells, these transcription activators exerted simultaneous activation of multiple genes and orthogonal regulation of different genes in a ligand-dependent manner with minimal background. We envision that our system will enable the perturbation of higher order gene networks with high temporal resolution and accelerate our understanding of gene-gene interactions in a complex biological setting.

Keywords: CRISPR/Cas9, synthetic transcription factor, chemically induced dimerization, genetic regulation, orthogonality

INTRODUCTION

Transcription factors play a fundamental role in regulating cellular behavior and determining cell fate. In mammalian cells, certain combinations of naturally existing transcription factors induce trans-differentiation and reprogramming, generating cells with therapeutic potential.[1] Synthetic transcription factors (sTFs) are artificial proteins that consist of a DNA binding domain and a trans-regulating effector domain. sTFs are a valuable synthetic biology tool and have been used in a variety of applications, including compensating for gene dysfunction,[2] controlling stem cell differentiation,[3] stimulating tissue regeneration,[4] performing gain-of-function screens,[5] and creating synthetic gene circuits.[6] Recently, the RNA-guided nuclease-deficient Cas9 (dCas9) protein from the type II Clustered, Regularly Interspaced Short Palindromic Repeats (CRISPR)/CRISPR-associated proteins (Cas) system has become a popular choice of DNA binding domain due to its ease-of-use and cost-effectiveness. Simply by changing the targeting sequence of the synthetic guide RNA (gRNA), the DNA binding specificity of dCas9 can be customized.[7, 8] Various synthetic transactivation domains have also been engineered to create constitutive dCas9 activators that activate endogenous human gene expression.[9]

Despite their high efficiency in activating silent genes, constitutive dCas9 activators do not allow temporal control over their function. This layer of control is necessary in resetting, fine-tuning and orchestrating complex cellular processes that occur in a time-dependent manner. Researchers have used inducible-promoter-driven Cas9 for gene-editing applications,[10] where the transcription of Cas9 mRNA only starts in the presence of a small molecule doxycycline. In theory, this approach can be extended to achieve inducible gene regulation. However, the inducible promoter suffered from leaky expression in the absence of doxycycline, which may lead to undesired gene activation. A conditionally stabilized dCas9 activator[11] and a split-dCas9 based activator[12] have also been engineered to respond to chemical ligands. However, in both cases undesired gene activation was detected in the absence of ligands, which may be due to the incomplete degradation of dCas9 activator or incomplete dissociation of split-dCas9 in the absence of ligands. On the other hand, coordinated regulation of multiple genes is still challenging due to the lack of robust designs for orthogonal control of sTFs. Since various chemically induced dimerization

(CID) systems[13, 14] and type II CRISPR/Cas systems[15] have been characterized, it should be possible to develop orthogonal chemically induced transcription factors for regulating multiple genes.

In this work, we developed inducible CRISPR/Cas9 activators with minimal background gene expression by expressing dCas9 and the transactivation domain on two separate peptides, which only dimerize in the presence of a chemical ligand. In addition, by combining orthogonal CID systems and orthogonal RNA-guided dCas9 proteins, we created inducible and orthogonal CRISPR/Cas9 activators and applied them to temporally regulate multiple endogenous human genes.

RESULTS AND DISCUSSION

To create tightly controlled CRISPR/Cas9 activators, each ligand binding domain (LBD) in a chemically induced dimerizing protein pair is fused separately with either dCas9 or the transactivation domain. In the absence of the chemical ligand, the transactivation domain is not recruited to the target gene, thus undesired gene activation should not be observed. In the presence of the ligand, two LBDs dimerize and the transactivation domain is recruited to the dCas9-bound target gene and activates its expression (Fig. 1). When the chemical ligand is removed from the system, the transactivation domain dissociates from dCas9 and stops activating the target gene. Two inducible CRISPR/Cas9 activators can function independently on two target genes due to the orthogonality between the two systems.

As proof-of-concept, we selected two commonly used Cas9 orthologs from *Streptococcus pyogenes* (referred to as $Cas9_{SP}$) and *Neisseria meningitidis* (referred to as $Cas9_{NM}$) to realize orthogonal regulation of two genes. Nuclease-deficient forms of $Cas9_{SP}$ (with amino acid substitutions D10A and H840A) and $Cas9_{NM}$ (with amino acid substitutions D16A, D587A, H588A, and N611A) have been characterized and shown to activate gene expressions in human cells when fused with a viral transactivation domain VP64.[7, 8, 15] We first explored whether enhanced activation can be achieved when VP64 was replaced with a recently reported synthetic transactivation domain VPR,[16] which is a fusion of three transactivation domains including VP64. Activation efficiencies of enhanced GFP (eGFP) reporters with four different

target sequences were compared (Fig. S1). $dCas9_{SP}$-VPR outperformed $dCas9_{SP}$-VP64 on all four targets with the same protospacer adjacent motif (PAM) sequence AGG (Fig. S1B). For $dCas9_{NM}$, we tested four different PAMs that have been previously reported to be functional.[17, 18] $dCas9_{NM}$-VPR outperformed $dCas9_{NM}$-VP64 on targets with PAM sequence AGGTGATT or AGGTGCTT (Fig. S1C). However, both $dCas9_{NM}$ activators failed to activate eGFP expression when PAM sequence AGGTGGTT or AGGTGTTA was used. Overall, VPR was confirmed to be a more efficient activator domain than VP64 and was used as the transactivation domain in the following experiments.

We then evaluated the orthogonality between the two Cas9 proteins for regulating multiple genes. To be orthogonal, a Cas9 ortholog must only recognize its own cognate gRNA and PAM sequence. We constructed an eGFP reporter plasmid with seven copies of identical target sequence that contains both PAM sequences for $dCas9_{SP}$ and $dCas9_{NM}$. We tested eGFP activation by different dCas9-VPR/gRNA combinations. Only combinations of dCas9-VPR and gRNA from the same species activated eGFP expression (Fig. S2). This observation is consistent with a previous study[15], suggesting that $dCas9_{SP}$ and $dCas9_{NM}$ are fully orthogonal to each other and can be used to bind to different target sites within the same genome.

We further selected gRNA targeting sequences for efficient activation of four endogenous human genes: *ASCL1*, *TTN*, *IL1RN* and *RHOXF2* (Supplementary text, Table S1, Fig. S3). The selected genes are normally expressed in different tissues but repressed in HEK293T cells. To enable an orthogonal control, the gRNAs targeting *ASCL1* and *IL1RN* were designed to be recognized by $dCas9_{SP}$, while the gRNAs targeting *TTN* and *RHOXF2* were designed to be recognized by $dCas9_{NM}$. Efficient gRNAs for each gene (gRNAs 130 for *ASCL1*; 29, 113, 145, and 180 for *IL1RN*; 68 for *TTN*; 148 and 302 for *RHOXF2*, Table S1) were used for the following experiments.

Different configurations of LBD-fused dCas9 activators were then characterized. We utilized two CID protein pairs, gibberellin-induced GAI/GID1 and rapamycin-induced FKBP/FRB (Fig. 1), that have been

previously shown to be orthogonal and used for constructing logic gates in living mammalian cells.[19] We fused one copy of GAI to the C-terminus of $dCas9_{SP}$ and one copy of GID1 to the N-terminus of VPR, and tested activation of an eGFP reporter gene under two different concentrations of a gibberellin analog GA_3-AM, as previously reported.[19] Similar levels of eGFP activation were observed with 10 μM and 100 μM GA_3-AM induction. When GID1 is fused to $dCas9_{SP}$ and GAI is fused to VPR, a decreased level of eGFP activation was observed under both GA_3-AM concentrations (Fig. S4). As a result, we used $dCas9_{SP}$-GAI/GID1-VPR pair and 10 μM GA_3-AM to activate endogenous *ASCL1* expression in HEK293T cells. However, no significant gene activation was observed (Fig. 1A). Previous study on the FKBP/FRB dimerization system concluded that fusing multiple copies of FKBP to the DNA binding domain may recruit more copies of FRB-fused activation domain, leading to an increased gene activation efficiency.[20] Adopting the same principle, we tested up to four copies of GAI fused to $dCas9_{SP}$. The highest activation efficiency was achieved when three copies of GAI were used (Fig. 1A). Since multiple copies of FKBP fused to the DNA binding domain was shown to work well,[20] we fused two copies of FKBP to the C-terminus of $dCas9_{SP}$ and one copy of FRB to the N-terminus of VPR. A rapamycin analog (rapalog) concentration of 0.1 μM was sufficient to activate eGFP expression (Fig. S5). To create an orthogonal system to $dCas9_{SP}$-3×GAI/GID1-VPR, we fused two copies and three copies of FKBP to the C-terminus of $dCas9_{NM}$, and tested activation of endogenous *TTN* expression under 0.1 μM rapalog. Two copies and three copies of FKBP showed comparable levels of gene activation (Fig. 1B). To ensure the highest activation efficiencies and minimal protein sizes, which is desired for gene delivery, we used $dCas9_{SP}$-3×GAI/GID1-VPR and $dCas9_{NM}$-2×FKBP/FRB-VPR in the following experiments (Fig. S6).

A significant advantage of using dCas9 as DNA binding domain is the great ease of multiplexing.[21] By simply co-expressing multiple gRNAs targeting multiple genes, dCas9 activators can be recruited to multiple loci across the genome and activate expression of multiple genes simultaneously. This is particularly important in applications where multiple genes have to be activated to carry out a certain biological process.[1] To test the potential of activating multiple genes in a ligand-dependent manner, we transfected HEK293T cells with gRNAs targeting two different genes. We used $dCas9_{SP}$-3×GAI/GID1-VPR

for activating *ASCL1* and *IL1RN* (Fig. 2A), and dCas9$_{NM}$-2×FKBP/FRB-VPR for activating *TTN* and *RHOXF2* (Fig. 2B). Upon ligand addition, both pairs of genes were simultaneously activated. While in the absence of the ligand, the expression level of each gene was similar to the basal level observed in untransfected cells (Fig. 2 A and B). Thus, both dCas9$_{SP}$-3×GAI/GID1-VPR and dCas9$_{NM}$-2×FKBP/FRB-VPR can be used for activating multiple genes simultaneously and in a ligand-dependent manner. To realize the simultaneous activation of all four genes, we further designed gRNAs SP-TTN-68, SP-RHOXF2-144 and SP-RHOXF2-304 (Table S1) that target roughly the same regions as NM-TTN-68, NM-RHOXF2-148 and NM-RHOXF2-302, for activating *TTN* and *RHOXF2* using dCas9$_{SP}$ activators. In this case we used dCas9$_{SP}$-2×FKBP/FRB-VPR for simultaneous induction of all four genes by rapalog. Upon rapalog addition, activation of all four genes was observed with minimal background (Fig. 2C). Comparing these simultaneous activation experiments gives an indirect comparison between different dCas9 platforms and CID systems. The activation fold of *TTN* decreased in the four gene activation experiment as compared to that in the two gene activation experiment (Fig. 2), where different dCas9s but the same CID system were used. This may be due to a variety of reasons including dilution of the gRNA expression plasmid, gene-gene interactions or inefficiency of dCas9$_{SP}$ in binding to that particular target locus. However, the activation fold of *RHOXF2* was significantly increased when dCas9$_{NM}$ was replaced by dCas9$_{SP}$ (Fig. 2). These results suggest that different genes or target sites may have different preferences over different dCas9 platforms. On the other hand, the activation folds of *ASCL1* and *IL1RN* both increased when GAI/GID1 was replaced by FKBP/FRB, indicating that FKBP/FRB is a more efficient dimerizing system for recruiting the VPR domain.

Next, we sought to evaluate whether two genes can be orthogonally regulated by two different ligands. We transfected HEK293T cells with dCas9$_{SP}$-3×GAI/GID1-VPR, dCas9$_{NM}$-2×FKBP/FRB-VPR, and a mixture of gRNAs targeting two different genes. We tested orthogonal regulation of two pairs of genes, *ASCL1*/*TTN* and *IL1RN*/*RHOXF2*, where *ASCL1* and *IL1RN* were induced by GA$_3$-AM and *TTN* and *RHOXF2* were induced by rapalog. We then induced distinct gene expression patterns by adding either a single ligand or both ligands (Fig. 3). For *ASCL1*/*TTN* gene pair, only *ASCL1* expression level increased upon GA$_3$-AM

addition, while only *TTN* expression level increased upon rapalog addition. When both ligands were added, both *ASCL1* and *TTN* expression levels increased (Fig. 3A). The activation efficiencies of *ASCL1* and *TTN* with addition of a single ligand both decreased as compared to the experiments when only one CRISPR/Cas9 activator system was transfected (Fig. 1 A and B). This may be due to the reduced amount of transfected plasmids expressing each system, as was observed in a previous study.[8] For the *IL1RN*/*RHOXF2* gene pair, an orthogonal regulation was also achieved under similar experimental settings (Fig. 3B). For both gene pairs, it was observed that the activation efficiencies decreased when both ligands were added, which may be due to additive toxic effects to the cells. To further demonstrate the ability of our systems to induce dynamic gene expression patterns, we monitored expression of *ASCL1* and *TTN* for three days post-transfection, during which GA_3-AM or rapalog were added upon different days (Fig. 4A). In one experiment, GA_3-AM was present during day 2 post-transfection. At the end of day 2, GA_3-AM was washed away and rapalog was added and kept present during day 3 post-transfection. In this scenario, the activation of *ASCL1* was observed after 24 hours induction with GA_3-AM, and then reversed when GA_3-AM was washed away. On the other hand, no significant activation of *TTN* was observed at the end of day 2. After induction with rapalog for 24 hours, the activation of *TTN* was observed (Fig. 4B upper panel). In another experiment, the sequence of GA_3-AM and rapalog addition was reversed. In this scenario, the activation of *ASCL1* was only observed during day 3 post-transfection, while the activation of *TTN* was observed during day 2 post-transfection, and reversed during day 3 post-transfection when rapalog was washed away (Fig. 4B lower panel). The results above collectively demonstrated that the two CRISPR/Cas9 activator systems developed in this study can be used for orthogonal and temporal regulation of multiple genes.

In this work, we developed two chemically inducible and orthogonal CRISPR/Cas9 activators by combining orthogonal CRISPR/Cas9 systems and orthogonal CID systems. These activators enabled temporal regulation of multiple genes. By physically dissociating dCas9 and the transactivation domain in the absence of the ligand, these activators induced expression of endogenous human genes with minimal

background, which is challenging for previous designs.[10-12] Furthermore, coordinated regulation of multiple endogenous human genes was realized through the use of orthogonal ligands.

The major application of our system is to regulate multiple genes in a time-dependent manner. This could have many applications in terms of studying gene functions. For example, by simultaneously activating multiple genes, functional interactions between different genes in a certain developmental stage can be studied. By fine-tuning the ligand doses or repeatedly switching between different ligands, it is also possible to study phenotypic consequences of complex genetic perturbations that are difficult to achieve with current technologies. Given the ease of multiplex targeting, it is also possible to orthogonally regulate multiple groups of genes.

In comparison with the light-induced CRISPR/Cas9 activators,[22, 23] more CID systems are available[14] as compared with light activated proteins, which is important when regulating higher order regulatory networks. With the characterization of a growing number of CRISPR systems,[24] it should be possible to scale up the number of genes that can be orthogonally regulated, enabling a more sophisticated regulation of gene networks. During the review process of this work, a similar work was published demonstrating orthogonal and inducible regulation of two genes by using dCas9 from *Staphylococcus aureus* and an abscisic acid inducible ABI/PYL1 CID system in addition to $dCas9_{SP}$ and GAI/GID1 CID system[25]. This study complemented with our work, collectively showing that the number of orthogonally controlled genes can be scaled up. In their work, FKBP/FRB system was also tested but was concluded to be less potent than GAI/GID1 system. While in our work, FKBP/FRB was shown to be more potent than GAI/GID1, possibly due to the multiple copies of LBDs used in our contructs. The orthogonal regulation of different genes has also been reported by using programmable RNA scaffolds.[26] It is likely that chemical induction of orthogonal gene activation can be achieved via RNA scaffolds, by fusing CID proteins to RNA binding proteins. In such cases, a single Cas9 ortholog will be sufficient for orthogonal regulation of multiple genes.

Besides gene activation, our system can also be used to induce gene repressions, epigenetic modifications[27] and precise genome editing[28] by replacing activation domain with suitable effector domains, thus enabling coordinated control of distinct biological processes. For example, the consequences of simultaneous gene editing and regulation can be studied. By replacing the effector domain with another DNA binding domain such as another dCas9 ortholog, it is possible to tether two remote genomic loci and study the effects of altered genome architecture in a reversible manner. We envision our systems to be useful for studies in both basic and applied science where coordinated regulation of multiple biological processes is needed.

METHODS

Plasmid construction. Plasmid pcDNA-dCas9-VP64 expressing dCas9$_{SP}$-VP64 was purchased from Addgene (Addgene plasmid 47107). All pcDNA plasmids were assembled using In-Fusion HD cloning kit (Clontech Laboratories). Plasmid pcDNA-dCas9$_{SP}$-VPR was made by assembling a PCR amplified VPR fragment with *Asc*I/*Pac*I digested pcDNA-dCas9-VP64 backbone. Plasmids pcDNA-dCas9$_{SP}$-2×FKBP, pcDNA-dCas9$_{SP}$-GAI, and pcDNA-dCas9$_{SP}$-GID1 were made by assembling PCR amplified 2×FKBP, GAI, and GID1 fragments with *Asc*I/*Xba*I digested pcDNA-dCas9-VP64 backbone, respectively. Plasmid pcDNA-dCas9$_{SP}$-2×GAI was made by assembling a PCR amplified GAI fragment with *Asc*I digested pcDNA-dCas9$_{SP}$-GAI. Repeating this process generated pcDNA-dCas9$_{SP}$-3×GAI and pcDNA-dCas9$_{SP}$-4×GAI. Plasmid pcDNA-dCas9$_{NM}$-VP64 was made by assembling a PCR amplified dCas9$_{NM}$ fragment with *Sac*II/*Bst*EII digested pcDNA-dCas9-VP64 backbone. Plasmid pcDNA-dCas9$_{NM}$-VPR was made by assembling a PCR amplified VPR fragment with *Asc*I/*Pac*I digested pcDNA-dCas9$_{NM}$-VP64 backbone. Plasmid pcDNA-dCas9$_{NM}$-2×FKBP was made by assembling a PCR amplified dCas9$_{NM}$ fragment with *Cla*I/*Bst*EII digested pcDNA-dCas9$_{SP}$-2×FKBP backbone. Plasmid pcDNA-dCas9$_{NM}$-3×FKBP was made by assembling a PCR amplified FKBP fragment with *Asc*I digested pcDNA-dCas9$_{NM}$-2×FKBP. Plasmids pcDNA-FRB-VPR, pcDNA-GAI-VPR, and pcDNA-GID1-VPR were made by assembling PCR amplified FRB, GAI and GID1 fragments with *Sac*II/*Bst*EII digested pcDNA-dCas9$_{SP}$-VPR backbone, respectively. Plasmid pSPgRNA expressing a *S. pyogenes* gRNA was

purchased from Addgene (Addgene plasmid 47108). A 20bp guide sequence was cloned into pSPgRNA by annealing and phosphorylating two complementary oligonucleotides 5'-caccgN(20)-3' and 5'-aaacN(20)c-3', then ligating into a *Bbs*I digested pSPgRNA backbone. N(20) represents the 20bp guide sequence. Plasmid pNMgRNA expressing a *N. meningitidis* gRNA was made by assembling a gBlock fragment (Integrated DNA Technologies) containing a hU6 promoter, two *Bbs*I sites and a *N. meningitidis* gRNA structural part with *Nde*I/*Sac*I digested pSPgRNA backbone using In-Fusion HD cloning. A 23bp guide sequence was cloned into pNMgRNA by annealing and phosphorylating two complementary oligonucleotides 5'-caccgN(23)-3' and 5'-caacN(23)c-3', then ligating into a *Bbs*I digested pNMgRNA backbone. All guide sequences used in this study are summarized in Table S1. All eGFP reporter plasmids with different target sites were generated by annealing and phosphorylating two complementary oligonucleotides containing seven copies of target sites, then ligating into a *Xma*I/*Bgl*II digested pGL3-Basic-9×Seq2-hCMVmp-eGFP plasmid[29] backbone. All plasmids generated in this study will be deposited with Addgene.

Cell culture, transfections and induction. HEK293T cells were maintained in DMEM (UIUC Cell Media Facility) supplemented with 10% FBS and 1% penicillin/streptomycin at 37°C in a humidified 5% CO_2 incubator. For transfections, 9×10^4 cells were plated per well of a 24-well plate. In 24 hours after plating, cells were transfected with Lipofectamine 2000 (Invitrogen) using 5 µl reagent per well. For activating reporter genes using constitutive dCas9 activators, each well was transfected with 50 ng, 117.5 ng, 200 ng and 82.5 ng of eGFP reporter plasmid, dCas9-VP64/VPR plasmid, gRNA expressing plasmid and a stuffer plasmid pCMV5, respectively. For activating reporter genes using inducible dCas9 activators, each well was transfected with 50 ng, 117.5 ng, 200 ng and 82.5 ng of eGFP reporter plasmid, dCas9-LBD plasmid, gRNA expressing plasmid, and LBD-VPR plasmid, respectively. A well transfected with 50 ng of eGFP reporter plasmid and 400 ng of pCMV5 was used to determine basal eGFP expression level. For activating a single endogenous gene using constitutive dCas9 activators, each well was transfected with 250 ng and 200 ng of dCas9-VPR plasmid and gRNA expression plasmids, respectively. For activating a single endogenous gene using inducible dCas9 activators, each well was transfected with 150 ng, 100 ng and

200 ng of dCas9-LBD plasmid, LBD-VPR plasmid, and gRNA expression plasmids, respectively. Equal amounts of gRNA expression plasmids were pooled to a total amount of 200 ng if multiple gRNAs were used to target the same gene. For activating multiple genes simultaneously, equal amounts of gRNA expression plasmids targeting each gene were pooled to a total amount of 200 ng. Different gRNA expression plasmids targeting the same gene were further sub-pooled in this case. For orthogonal regulation of two genes, each well was transfected with 75 ng, 50 ng and 100 ng of each dCas9-LBD plasmid, LBD-VPR plasmid and gRNA expression plasmids, respectively. In 24 hours after transfection, cells were induced with fresh media supplemented with appropriate ligands. For dynamic regulation experiments, cells were washed with PBS three times on day 2 post-transfection before addition of ligand-supplemented media. A stock of 5 mM GA_3-AM in DMSO and a stock of 0.05 mM rapalog (Clontech Laboratories) in DMSO were used to make working concentrations.

Flow cytometry. For comparing VP64 and VPR, cells were collected 24 hours after transfection. For all other experiments, cells were collected 48 hours after transfection. Collected cells were resuspended in 300 µl PBS + 0.5 mM EDTA to prepare flow cytometry samples. Samples were analyzed on a LSR II Flow Cytometer (BD Biosciences). Arithmetic mean of eGFP fluorescence was used to calculate fold activation comparing to a reporter only control.

Quantitative real time PCR. Cells were collected in 48 hours or on appropriate days after transfection. RNA was purified using the RNeasy mini kit (Qiagen) with RNase free DNase treatment. cDNA was synthesized from 1 µg RNA using the iScript cDNA synthesis kit (Bio-Rad). 1 µl of cDNA was used for each qPCR reaction, using the iQ SYBR Green Supermix (Bio-Rad). qPCR primers for *ACTB*, *ASCL1*, *IL1RN* and *TTN* were previously reported. qPCR primers for *RHOXF2* were designed using Primer3Plus (http://primer3plus.com/cgi-bin/dev/primer3plus.cgi). All qPCR primers are listed in Table S2. qPCR was run with three technical replicates on the 7900HT Fast Real-Time PCR System (Applied Biosystems) with 40 amplification cycles. Ct values were derived from the log phase of PCR using a threshold of 12 and a baseline of 1 to 10 in the SDS software (version 2.4.1, Applied Biosystems). Outliers within the three

technical replicates were removed. dCas9-VPR activated samples were used to construct qPCR standard curves (Fig. S7), from which relative gene expression levels were calculated. Relative gene expression levels of technical replicates were then averaged. All gene expression levels of *ASCL1*, *IL1RN*, *TTN* and *RHOXF2* were normalized to the expression levels of *ACTB*. To account for variations in basal gene expression levels, 11 independent biological replicates of *ASCL1*, *IL1RN*, *TTN* and 10 independent biological replicates of *RHOXF2* were tested and the average values were used as basal gene expression levels. Genes failed to amplify within 40 cycles were considered not expressed.

Statistical analysis. Data is shown as mean ± s.e.m, with biological replicate numbers indicated in the figure legends. All *P* values were generated from two-tailed *t*-tests using the GraphPad Prism software package (version 6.0c, GraphPad Software).

SUPPORTING INFORMATION

Supplementary text, figures and tables as described in the text. This material is available free of charge via the Internet at http://pubs.acs.org.

AUTHOR INFORMATION

Author Contribution

Z.B. and H.Z. designed the research. Z.B. performed the experiments, and S.J. and V.J. assisted with plasmid construction. Z.B. analyzed the data. H.Z. supervised the research. Z.B. and H.Z. wrote the manuscript.

Conflict of Interest

The authors declare no competing financial interest.

ACKNOWLEDGEMENTS

The authors thank Dr. Charles A. Gersbach (Department of Biomedical Engineering, Duke University, Durham, North Carolina, USA) for sharing plasmid pGL3-Basic-9×Seq2-hCMVmp-eGFP, Dr. Takanari Inoue (Department of Cell Biology, Center for Cell Dynamics, School of Medicine, Johns Hopkins University, Baltimore, Maryland, USA) for sharing plasmids CFP-GAI(1-92) and YFP-GID1, Dr. Tasuku Ueno (Laboratory of Chemistry and Biology, Graduate School of Pharmaceutical Sciences, The University of Tokyo, Tokyo, Japan) for providing ligand GA_3-AM. This work was supported by the Carl R. Woese Institute for Genomic Biology at the University of Illinois at Urbana-Champaign.

REFERENCES

1. Graf, T. (2011) Historical origins of transdifferentiation and reprogramming, *Cell Stem Cell 9*, 504-516.
2. Graslund, T., Li, X., Magnenat, L., Popkov, M., and Barbas, C. F., 3rd. (2005) Exploring strategies for the design of artificial transcription factors: targeting sites proximal to known regulatory regions for the induction of gamma-globin expression and the treatment of sickle cell disease, *J. Biol. Chem. 280*, 3707-3714.
3. Bartsevich, V. V., Miller, J. C., Case, C. C., and Pabo, C. O. (2003) Engineered zinc finger proteins for controlling stem cell fate, *Stem Cells 21*, 632-637.
4. Rebar, E. J., Huang, Y., Hickey, R., Nath, A. K., Meoli, D., Nath, S., Chen, B., Xu, L., Liang, Y., Jamieson, A. C., Zhang, L., Spratt, S. K., Case, C. C., Wolffe, A., and Giordano, F. J. (2002) Induction of angiogenesis in a mouse model using engineered transcription factors, *Nat. Med. 8*, 1427-1432.
5. Konermann, S., Brigham, M. D., Trevino, A. E., Joung, J., Abudayyeh, O. O., Barcena, C., Hsu, P. D., Habib, N., Gootenberg, J. S., Nishimasu, H., Nureki, O., and Zhang, F. (2015) Genome-scale transcriptional activation by an engineered CRISPR-Cas9 complex, *Nature 517*, 583-588.
6. Lienert, F., Torella, J. P., Chen, J. H., Norsworthy, M., Richardson, R. R., and Silver, P. A. (2013) Two- and three-input TALE-based AND logic computation in embryonic stem cells, *Nucleic Acids Res. 41*, 9967-9975.
7. Perez-Pinera, P., Kocak, D. D., Vockley, C. M., Adler, A. F., Kabadi, A. M., Polstein, L. R., Thakore, P. I., Glass, K. A., Ousterout, D. G., Leong, K. W., Guilak, F., Crawford, G. E., Reddy, T. E., and Gersbach, C. A. (2013) RNA-guided gene activation by CRISPR-Cas9-based transcription factors, *Nat. Methods 10*, 973-976.
8. Maeder, M. L., Linder, S. J., Cascio, V. M., Fu, Y., Ho, Q. H., and Joung, J. K. (2013) CRISPR RNA-guided activation of endogenous human genes, *Nat. Methods 10*, 977-979.
9. Chavez, A., Tuttle, M., Pruitt, B. W., Ewen-Campen, B., Chari, R., Ter-Ovanesyan, D., Haque, S. J., Cecchi, R. J., Kowal, E. J., Buchthal, J., Housden, B. E., Perrimon, N., Collins, J. J., and Church, G. (2016) Comparison of Cas9 activators in multiple species, *Nat. Methods 13*, 563-567.
10. Dow, L. E., Fisher, J., O'Rourke, K. P., Muley, A., Kastenhuber, E. R., Livshits, G., Tschaharganeh, D. F., Socci, N. D., and Lowe, S. W. (2015) Inducible in vivo genome editing with CRISPR-Cas9, *Nat. Biotechnol. 33*, 390-394.
11. Balboa, D., Weltner, J., Eurola, S., Trokovic, R., Wartiovaara, K., and Otonkoski, T. (2015) Conditionally Stabilized dCas9 Activator for Controlling Gene Expression in Human Cell Reprogramming and Differentiation, *Stem Cell Reports 5*, 448-459.
12. Zetsche, B., Volz, S. E., and Zhang, F. (2015) A split-Cas9 architecture for inducible genome editing and transcription modulation, *Nat. Biotechnol. 33*, 139-142.
13. Fegan, A., White, B., Carlson, J. C., and Wagner, C. R. (2010) Chemically controlled protein assembly: techniques and applications, *Chem. Rev. 110*, 3315-3336.
14. Auslander, S., and Fussenegger, M. (2013) From gene switches to mammalian designer cells: present and future prospects, *Trends Biotechnol. 31*, 155-168.

15. Esvelt, K. M., Mali, P., Braff, J. L., Moosburner, M., Yaung, S. J., and Church, G. M. (2013) Orthogonal Cas9 proteins for RNA-guided gene regulation and editing, *Nat. Methods 10*, 1116-1121.
16. Chavez, A., Scheiman, J., Vora, S., Pruitt, B. W., Tuttle, M., E, P. R. I., Lin, S., Kiani, S., Guzman, C. D., Wiegand, D. J., Ter-Ovanesyan, D., Braff, J. L., Davidsohn, N., Housden, B. E., Perrimon, N., Weiss, R., Aach, J., Collins, J. J., and Church, G. M. (2015) Highly efficient Cas9-mediated transcriptional programming, *Nat. Methods 12*, 326-328.
17. Hou, Z., Zhang, Y., Propson, N. E., Howden, S. E., Chu, L. F., Sontheimer, E. J., and Thomson, J. A. (2013) Efficient genome engineering in human pluripotent stem cells using Cas9 from Neisseria meningitidis, *Proc. Natl. Acad. Sci. U. S. A. 110*, 15644-15649.
18. Ma, H., Naseri, A., Reyes-Gutierrez, P., Wolfe, S. A., Zhang, S., and Pederson, T. (2015) Multicolor CRISPR labeling of chromosomal loci in human cells, *Proc. Natl. Acad. Sci. U. S. A. 112*, 3002-3007.
19. Miyamoto, T., DeRose, R., Suarez, A., Ueno, T., Chen, M., Sun, T. P., Wolfgang, M. J., Mukherjee, C., Meyers, D. J., and Inoue, T. (2012) Rapid and orthogonal logic gating with a gibberellin-induced dimerization system, *Nat. Chem. Biol. 8*, 465-470.
20. Rivera, V. M., Berk, L., and Clackson, T. (2012) Dimerizer-mediated regulation of gene expression, *Cold Spring Harb. Protoc. 2012*, 767-770.
21. Bao, Z., Cobb, R. E., and Zhao, H. (2016) Accelerated genome engineering through multiplexing, *Wiley Interdiscip. Rev. Syst. Biol. Med. 8*, 5-21.
22. Nihongaki, Y., Yamamoto, S., Kawano, F., Suzuki, H., and Sato, M. (2015) CRISPR-Cas9-based photoactivatable transcription system, *Chem. Biol. 22*, 169-174.
23. Polstein, L. R., and Gersbach, C. A. (2015) A light-inducible CRISPR-Cas9 system for control of endogenous gene activation, *Nat. Chem. Biol. 11*, 198-200.
24. Makarova, K. S., Wolf, Y. I., Alkhnbashi, O. S., Costa, F., Shah, S. A., Saunders, S. J., Barrangou, R., Brouns, S. J., Charpentier, E., Haft, D. H., Horvath, P., Moineau, S., Mojica, F. J., Terns, R. M., Terns, M. P., White, M. F., Yakunin, A. F., Garrett, R. A., van der Oost, J., Backofen, R., and Koonin, E. V. (2015) An updated evolutionary classification of CRISPR-Cas systems, *Nat. Rev. Microbiol. 13*, 722-736.
25. Gao, Y., Xiong, X., Wong, S., Charles, E. J., Lim, W. A., and Qi, L. S. (2016) Complex transcriptional modulation with orthogonal and inducible dCas9 regulators, *Nat. Methods 13*, 1043-1049.
26. Zalatan, J. G., Lee, M. E., Almeida, R., Gilbert, L. A., Whitehead, E. H., La Russa, M., Tsai, J. C., Weissman, J. S., Dueber, J. E., Qi, L. S., and Lim, W. A. (2015) Engineering complex synthetic transcriptional programs with CRISPR RNA scaffolds, *Cell 160*, 339-350.
27. Hilton, I. B., D'Ippolito, A. M., Vockley, C. M., Thakore, P. I., Crawford, G. E., Reddy, T. E., and Gersbach, C. A. (2015) Epigenome editing by a CRISPR-Cas9-based acetyltransferase activates genes from promoters and enhancers, *Nat. Biotechnol. 33*, 510-517.
28. Komor, A. C., Kim, Y. B., Packer, M. S., Zuris, J. A., and Liu, D. R. (2016) Programmable editing of a target base in genomic DNA without double-stranded DNA cleavage, *Nature 533*, 420-424.
29. Polstein, L. R., and Gersbach, C. A. (2012) Light-inducible spatiotemporal control of gene

activation by customizable zinc finger transcription factors, *J. Am. Chem. Soc. 134*, 16480-16483.

FIGURE LEGENDS

Figure 1. Activation of endogenous human genes by orthogonal, chemically induced CRISPR/Cas9 activators. (A) Ligand-dependent activation of *ASCL1* using $dCas9_{SP}$ activators. Up to 4 copies of GAI were fused to the C-terminus of $dCas9_{SP}$ and 1 copy of GID1 was fused to the N-terminus of VPR. Upon GA_3 (cellular form of GA_3-AM) addition, GID1 dimerizes with GAI and VPR activated *ASCL1* expression. (B) Ligand-dependent activation of *TTN* using $dCas9_{NM}$ activators. 2 or 3 copies of FKBP were fused to the C-terminus of $dCas9_{NM}$ and 1 copy of FRB was fused to the N-terminus of VPR. Upon rapalog addition, FRB dimerizes with FKBP and VPR activated *TTN* expression. n = 3 biological replicates. Error bars represent standard error of the mean. Significance levels were determined versus uninduced samples. **, $P < 0.01$. ***, $P < 0.001$. ****, $P < 0.0001$.

Figure 2. Simultaneous induction of multiple endogenous human genes. (A) Simultaneous activation of *ASCL1* and *IL1RN* by $dCas9_{SP}$-3×GAI/GID1-VPR. (B) Simultaneous activation of *TTN* and *RHOXF2* by $dCas9_{NM}$-2×FKBP/FRB-VPR. For A and B, n = 5 biological replicates. (C) Simultaneous activation of four genes by $dCas9_{SP}$-2×FKBP/FRB-VPR. For C, n = 3 biological replicates. All error bars represent standard error of the mean. All significance levels were determined versus untransfected samples. *, $P < 0.05$. **, $P < 0.01$. ***, $P < 0.001$. ****, $P < 0.0001$.

Figure 3. Orthogonal regulation of two different genes. (A) Orthogonal regulation of *ASCL1* and *TTN*. *ASCL1* is activated in the presence of GA_3 (blue triangle), while *TTN* is activated in the presence of rapalog (yellow square). (B) Orthogonal regulation of *IL1RN* and *RHOXF2*. *IL1RN* is activated in the presence of GA_3, while *RHOXF2* is activated in the presence of rapalog. n = 3 biological replicates. All error bars represent standard error of the mean. All significance levels were determined versus untransfected samples. **, $P < 0.01$. ***, $P < 0.001$. ND, not detected.

Figure 4. Temporal regulation of two different genes. (A) Scheme showing temporal regulation of *ASCL1* and *TTN* by GA_3-AM and rapalog. In the presence of GA_3-AM (blue triangle), *ASCL1* is activated while *TTN* remains repressed. When GA_3-AM is replaced by rapalog (yellow square), *TTN* is activated while *ASCL1* becomes repressed. (B) Upper panel, GA_3-AM was added on day 1 post-transfection. On day 2 post-transfection, GA_3-AM was washed away and rapalog was added. Lower panel, rapalog was added on day 1 post-transfection. On day 2 post-transfection, rapalog was washed away and GA_3-AM was added. n = 3 biological replicates. All error bars represent standard error of the mean. All significance levels were determined versus untransfected samples except for day 3 *TTN* in lower panel, which is determined versus day 2 *TTN* in the same figure. *, $P < 0.05$. **, $P < 0.01$. ***, $P < 0.001$.

FIGURES

Figure 1

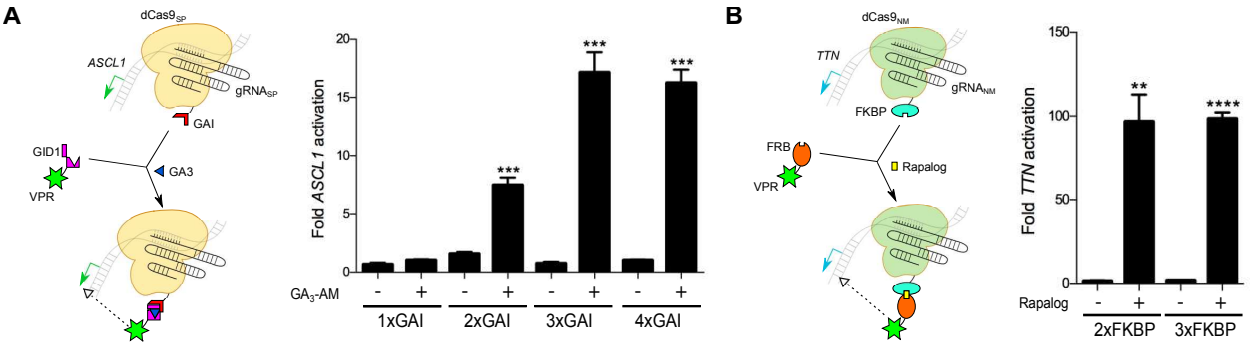


Figure 2

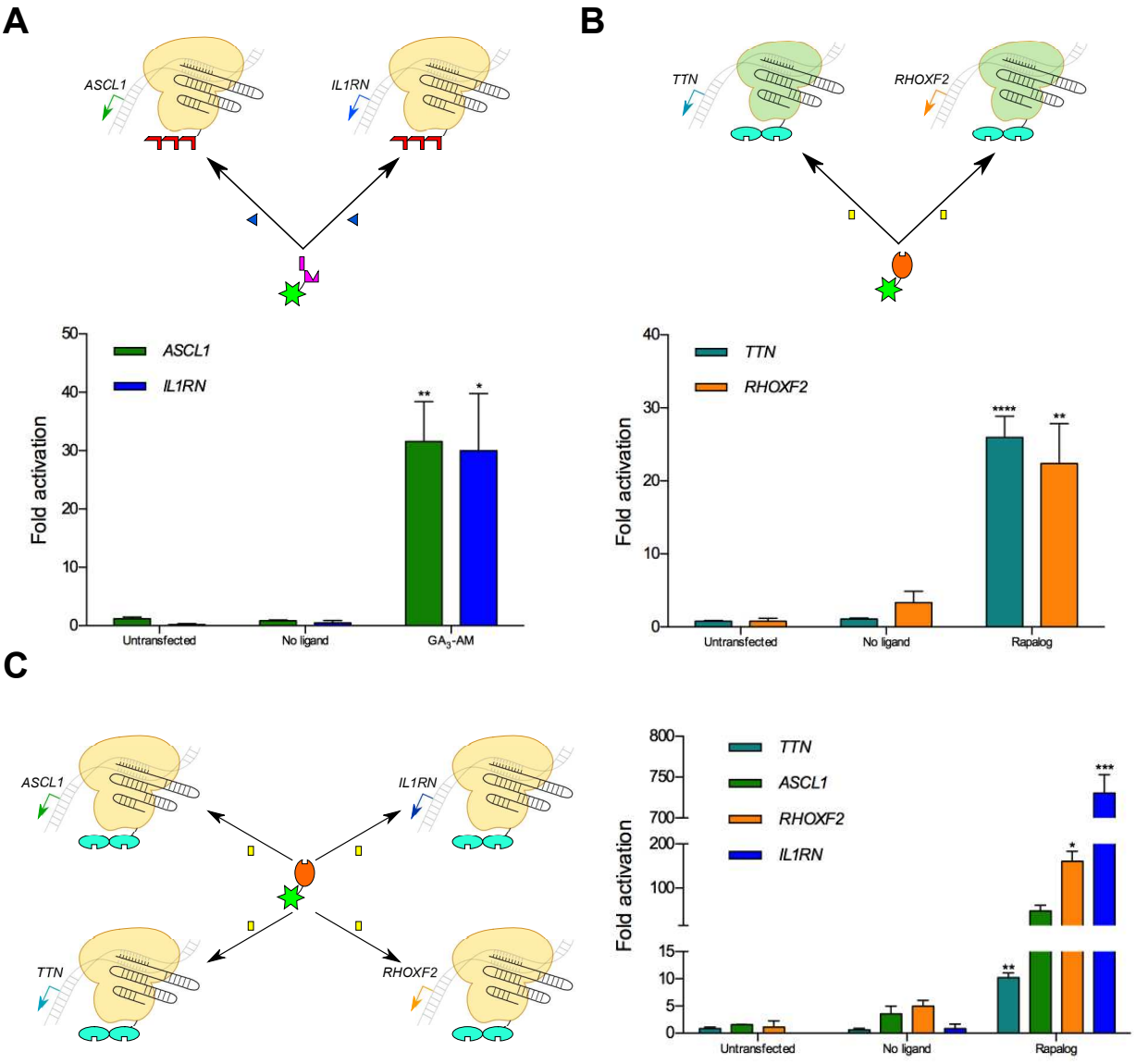

A
ASCL1
IL1RN
Fold activation
ASCL1
IL1RN
Untransfected
No ligand
GA3-AM
B
TTN
RHOXF2
Fold activation
TTN
RHOXF2
Untransfected
No ligand
Rapalog
C
ASCL1
IL1RN
TTN
RHOXF2
Fold activation
TTN
ASCL1
RHOXF2
IL1RN
Untransfected
No ligand
Rapalog

Figure 3

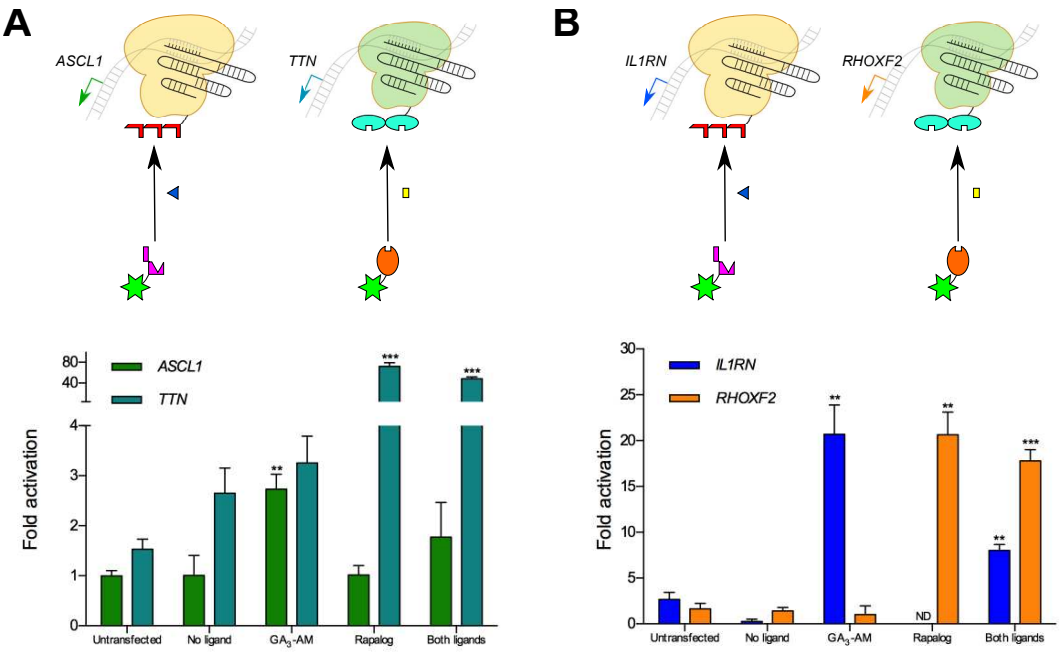
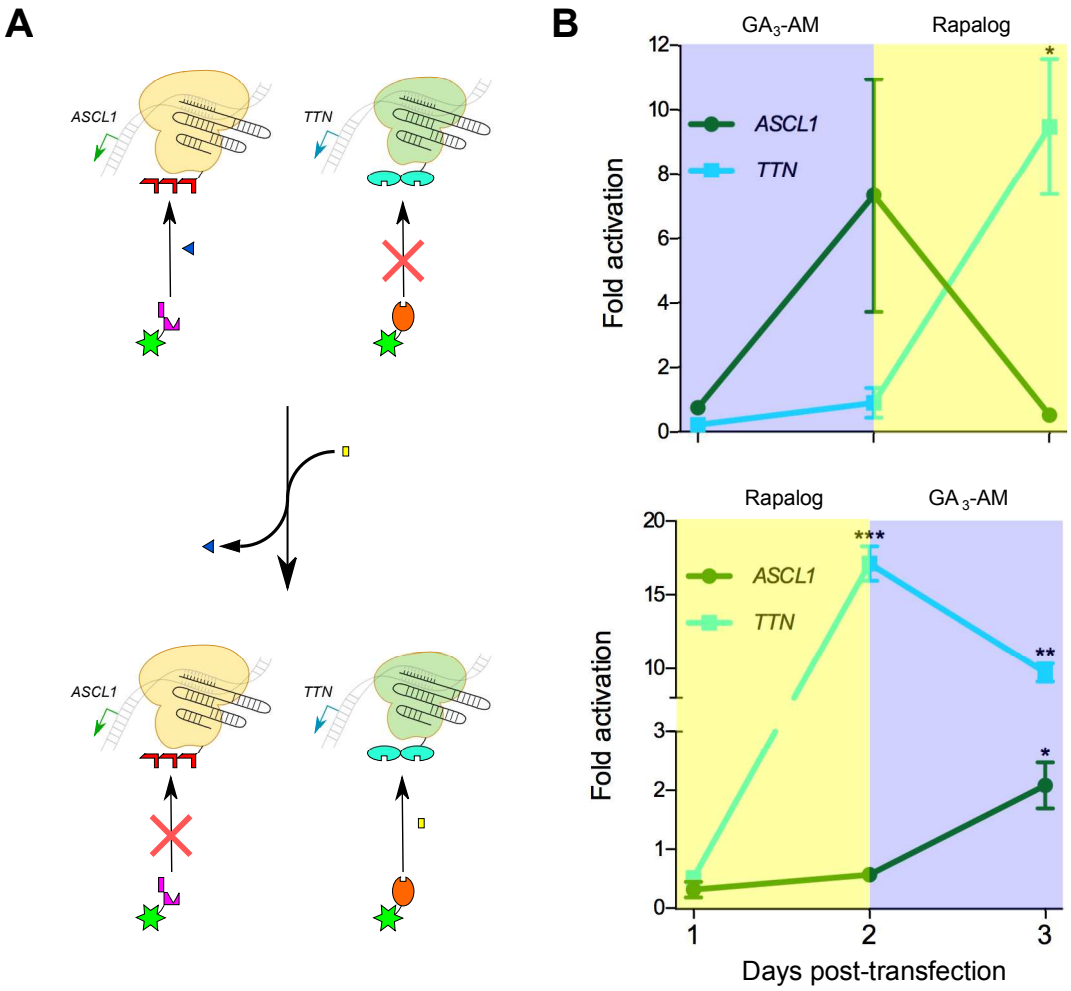
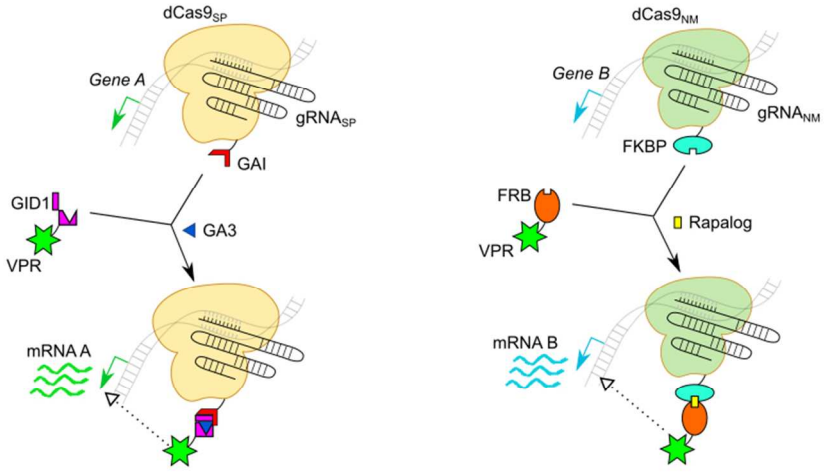

A
ASCL1
TTN
ASCL1
TTN
Fold activation
Untransfected
No ligand
GA3-AM
Rapalog
Both ligands
B
IL1RN
RHOXF2
IL1RN
RHOXF2
Fold activation
ND

Figure 4


A
ASCL1
TTN
ASCL1
TTN
B
GA3-AM
Rapalog
ASCL1
TTN
Fold activation
Rapalog
GA3-AM
ASCL1
TTN
Fold activation
Days post-transfection



TOC graphic

80x39mm (300 x 300 DPI)

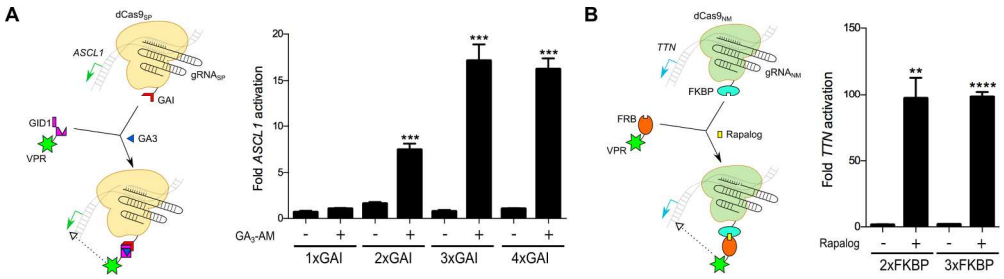


Figure 1

200x53mm (300 x 300 DPI)

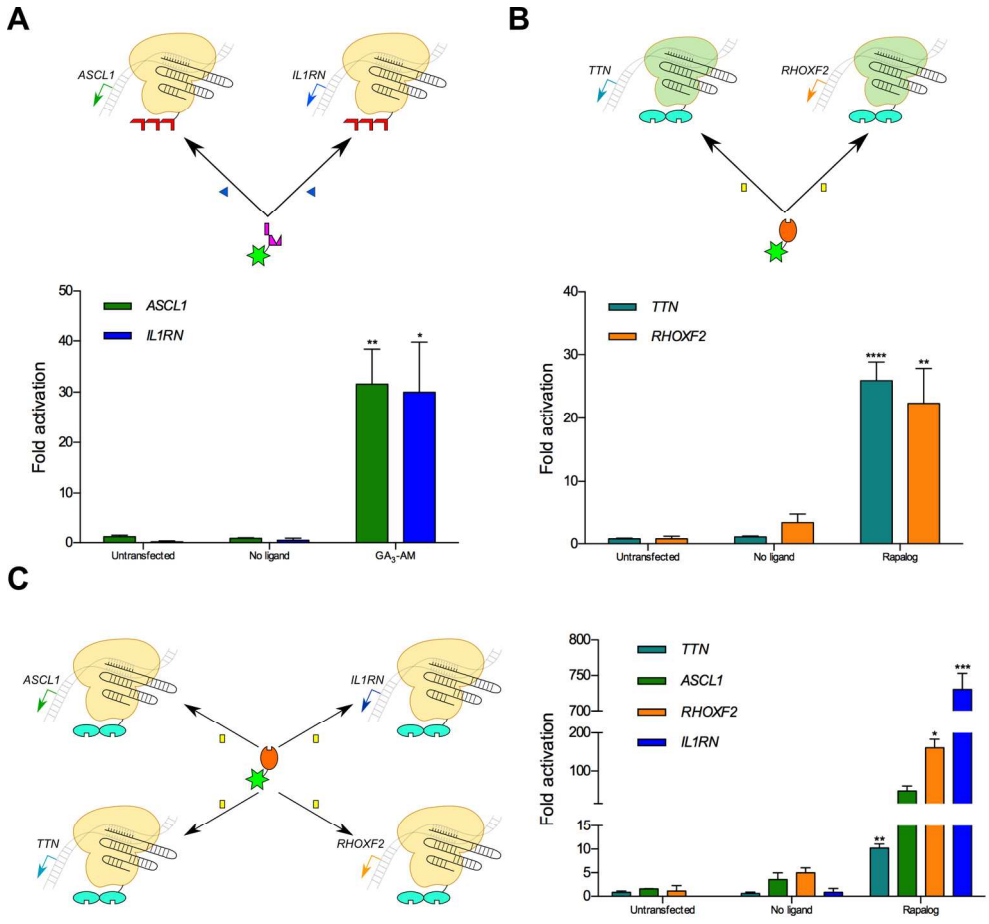


Figure 2

166x152mm (300 x 300 DPI)

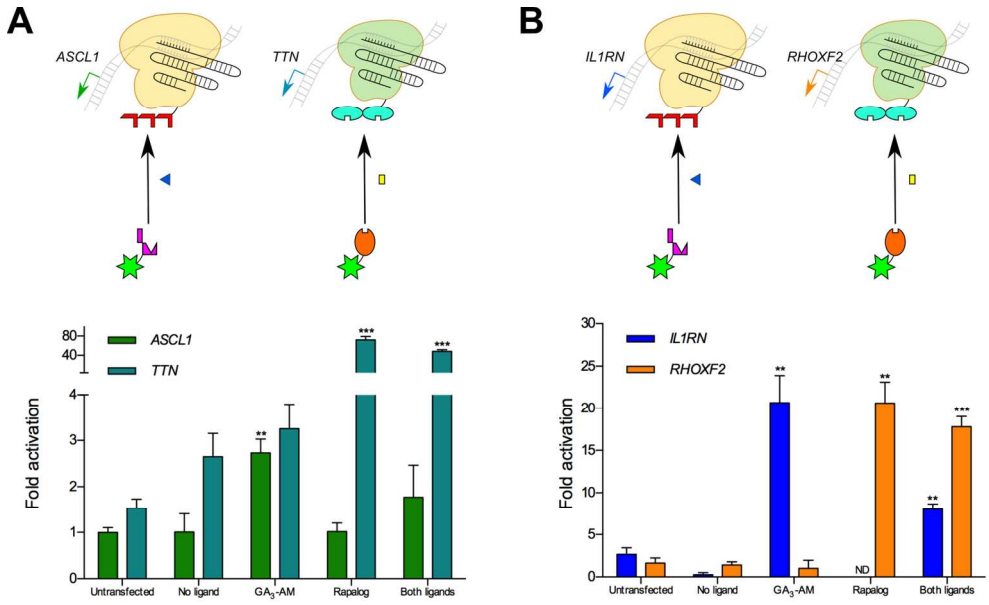


Figure 3

142x85mm (300 x 300 DPI)

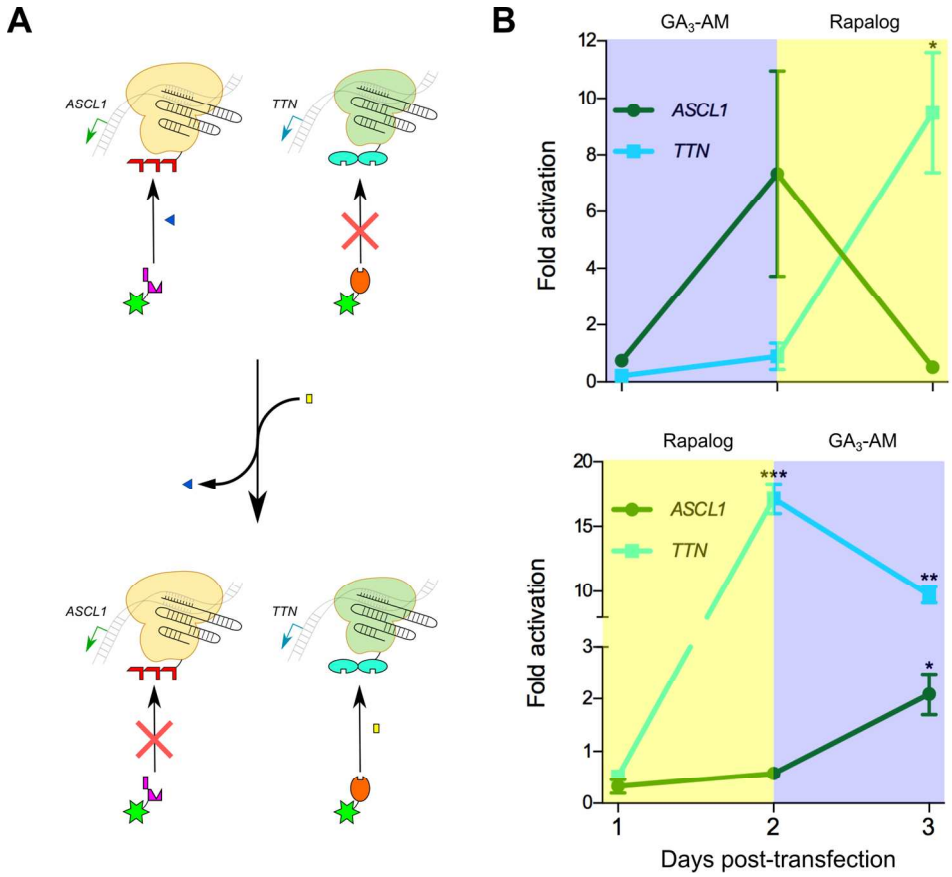


Figure 4

148x128mm (300 x 300 DPI)